Received: 5 July 2020 | Revised: 20 November 2020 | Accepted: 30 November 2020

IET Circuits, Devices & Systems

DOI: 10.1049/cds2.12045

The Institution of Engineering and Technology WILEY

ORIGINAL RESEARCH PAPER

Low pass filter design with improved stop-band suppression and synthesis with transformer-free ladders

Serkan Yildiz[1] | **Ahmet Aksen**[2] | **Sedat Kilinc**[3] | **Siddik B. Yarman**[3]

[1]The Scientific and Technological Research Council of Turkey, Kocaeli, Turkey

[2]Department of Electrical and Electronics Engineering, Faculty of Engineering, Isik University, Istanbul, Turkey

[3]Department of Electrical and Electronics Engineering, Faculty of Engineering, Istanbul University-Cerrahpasa, Istanbul, Turkey

Correspondence

Serkan Yildiz, The Scientific and Technological Research Council of Turkey, Kocaeli, Turkey.
Email: seryildiz@itu.edu.tr

Abstract

A new method to design transformer-free low pass (LP) ladder network with improved stop-band suppression performance is introduced. The parametric representation of back-end impedance of LP filter network is established with minimum impedance part and a Foster reactance part. The constructed impedance function is optimized by using real frequency technique. It has been shown that the proposed method provides LP filters which have superior stop-band suppression in comparison with classical transfer function-based filters with same complexity. The synthesis of the LP filter is obtained with the proposed element extraction procedure and resulted with fully realizable network elements in ladder form. An LP filter design and application by employing the proposed technique is provided. The measurement results of the prototyped filter are presented.

1 | INTRODUCTION

Low pass (LP) filter design is well elaborated in the filter literature. A well-known transfer function-based method such as Chebyshev, Elliptical, Bessel etc. can be incorporated to design and synthesize filter network [1,2]. The performance of the filter depends on the chosen transfer function and several input parameters such as degree of the filter, ripple level. However, the given filter performance might not satisfy the design requisites.

Besides of these methods, the front-end or back-end impedance or admittance of a LP lossless two-port network can be written in parametric form by setting the locations of transmission zeros and assigning the coefficients of the denominator polynomial. This provides a certain degree of freedom [3] to shape filter performance as it allows setting the location of transmission zeros, the degree of the network function, transfer characteristics, etc. Once the Brune function is determined, the filter network is synthesized by using lumped inductors and capacitors in series/shunt configuration [4,5], which is called ladder realization.

Transmission zero at DC (Direct Current) is synthesized as a series inductor or a shunt capacitor. Furthermore, each transmission zero at infinity is synthesized as shunt inductor and series capacitor [4–6]. The finite transmission zeros are synthesized as series/shunt resonator sections with partial cascading elements. One of the well-known topology is known as Brune section [5]. However, one of cascading element in Brune section always results with negative value, which is unrealizable.

In literature, several methods have been presented to eliminate these negative elements [6–8]. In one of the study [8], the driving point impedance of lossless two-port is constructed with a novel approach. It is represented with a Foster reactance part and a minimum impedance part and named as non-minimum impedance function. In this study, the well-known real frequency technique (RFT) are used to optimize the constructed impedance over the desired band of interest.

This method is re-visited and investigated its benefits on gain performance of a filter network. Using RFT with the proposed procedure, provides better convergence in optimization to increase suppression level at stop band and decrease the insertion loss level at pass band. Besides using transfer function based filters, this method provides a semi-analytical design procedure, which includes optimization routine and produces better filter characteristics than the classical transfer function-based filters. Due to the nature of the presented procedure, a degenerative gain response is expected. Here, it has been presented that this effect provides a superior stop-band suppression in comparison with transfer function-based filters with identical complexities. An LP filter design and its implementation results are presented to validate the proposed effect of this technique.

2 | PARAMETRIC REPRESENTATION OF NON-MINIMUM DRIVING-POINT IMPEDANCE

Consider the lossless two-port in Figure 1. The back-end driving point impedance $Z(p)$can be represented with minimum part and Foster reactance part as in (1).

$$Z(p) = \frac{n(p)}{d(p)} = Z_F(p) + Z_{\min}(p) \tag{1}$$

Foster reactance part is given in general form as [3]

$$Z_F(p) = k_\infty p + \frac{k_0}{p} + \sum_{i=1}^{N} \frac{k_i p}{p^2 + w_i^2} \tag{2}$$

where k_∞ is the residue of the pole at infinity, k_0 is the residue of the pole at zero and k_i is the residues at the complex conjugate poles located at $p = jw_i$. All the residues k_∞, k_0 and k_i must be real and non-negative [3].

The minimum impedance part which is also known as the positive real function or Brune function, is represented as (3)

$$Z_{\min}(p) = \frac{a(p)}{b(p)} = \frac{a_k p^k + a_{k-1}p^{k-1} + \ldots + a_1 p + a_0}{b_l p^l + b_{l-1}p^{l-1} + \ldots + b_1 p + b_0} \tag{3}$$

whose all poles must be placed at the left-hand plane and corresponding residues have to be positive [7]. The even part of the minimum impedance $Z_{\min}(p)$ is:

$$R(p) = \frac{F(p)}{b(p)b(-p)} \tag{4}$$

where roots of the $F(p)$ polynomial represent the transmission zeros of the lossless two-port network. This polynomial is given in general form as:

$$F(p) = a_0^2(-1)^{ndc} p^{ndc} \prod_{i=1}^{n_z} \left(p^2 + w_i^2\right)^2 \tag{5}$$

where a_0 is real arbitrary constant, ndc and n_z are the number of the transmission zeros at DC and at finite frequencies, respectively. The w_i is the location of the finite transmission zeros. The denominator of the even part in (4) can be represented as:

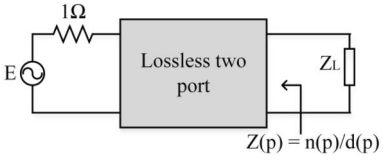

FIGURE 1 Lossless two-port network

$$b(p)b(-p) = \frac{1}{2}\left(c(p)^2 + c(-p)^2\right); n = \deg(b(p)) \tag{6}$$

where $c(p)$ is and arbitrary polynomial and n is the degree of $b(p)$ polynomial. The following relation is held between n, ndc and n_z as:

$$n = ndc + 2n_z + n_\infty \tag{7}$$

where the n_∞ represents the number of transmission zeros at infinity. Therefore, the minimum part impedance is explicitly defined in terms of transmission zeros and coefficients of $c(p)$ polynomial.

If the Foster part is composed of only a serial inductor whose inductance value is equal to $L = k_\infty$ then the first term of (2) will be enough to represent the Foster reactance part. Therefore, the back-end driving point impedance in (1) is simplified as

$$\begin{aligned} Z(p) &= \frac{n(p)}{d(p)} = pk_\infty + \frac{a(p)}{b(p)} = \frac{pk_\infty b(p) + a(p)}{b(p)} \\ &= \frac{n_n p^n + n_{n-1}p^{n-1} + \cdots + n_1 p + n_0}{d_m p^m + d_{m-1}p^{m-1} + \cdots + d_1 p + d_0} \end{aligned} \tag{8}$$

A transducer power gain (TPG) function can be determined in terms of real and imaginary part impedances of the load network and back-end impedance of the lossless two-port in Figure 1 as

$$TPG(w) = \frac{4R_G(w)R_L(w)}{\left(R_L(w) + R_G(w)\right)^2 + \left(X_L(w) + X_G(w)\right)^2} \tag{9}$$

In RFT procedure, the coefficients of the $c(p)$ polynomial are randomly initiated and by employing an optimization routine, these coefficients are iterated. In each cycle of the iteration, $Z(p)$ impedance is generated and $TPG(w)$ is calculated. Here, we fix the Foster part reactance and keep out the optimization routine. The following objective function is chosen to be minimized.

$$\delta(w) = \sum_{i=1}^{N_w} (TPG(w_i) - T_0(w_i)) \tag{10}$$

where N_w the number of breaking point frequencies and $T_0(w)$is target TPG level.

The output of the optimization is the coefficients of $c(p)$ polynomial. By using the optimized coefficients and substituting (4) to (6), the optimized $Z_{min}(p)$ is determined then the back-end driving point impedance $Z(p)$ in (8) is achieved.

The resultant impedance is synthesized with a prescribed element extraction procedure, which is presented in the following section.

3 | SYNTHESIS PROCEDURE OF THE DRIVING POINT IMPEDANCE

The determined impedance is synthesized with the zero-shifting extraction routine with a certain order. The topology of the network is initially determined by the $F(p)$ polynomial in (5). The number of transmission zeros and their locations are assigned by the designer.

Therefore, each transmission zero at DC is extracted as a series capacitor or shunt inductor. Each finite transmission zero is extracted as a Brune section [7,8] as illustrated in Figure 2. The remaining transmission zeros in infinity are extracted as shunt capacitor and series inductor.

One of those two L_a and L_c inductors always result with negative value. To eliminate the negative inductors of Brune section, there is a special order for extraction of transmission zeros. The synthesis starts with extracting Foster reactance part by using the following relation:

$$L = k_\infty = \frac{n_n}{d_m} \tag{11}$$

The remainder minimum part impedance is generated as:

$$Z_{\min}(p) = \frac{a(p)}{b(p)} = \frac{n(p) - pk_\infty d(p)}{d(p)} \tag{12}$$

The minimum part of the impedance is suitable for Brune section extraction. Therefore, at the second step of the synthesis procedure, all finite transmission zeros are extracted in cascaded manner. Brune section extraction from impedance is well-known in literature. The details can be found at [5]. In further steps, the transmission zeros at DC and infinity are extracted, respectively [4].

The outlined extraction procedure will lead a circuit topology as illustrated in Figure 3.

In this network topology, the negative and positive inductors at series arm of adjacent Brune sections are summed up. The first negative inductor L_{a1} is eliminated by summing with $L_{\inf}$. The final network will be composed of all positive realizable network elements.

The outlined semi-analytical approach has a certain ambiguity in the elimination of all negative elements. This method let us to define the value of the first inductor $L_{\inf}$.

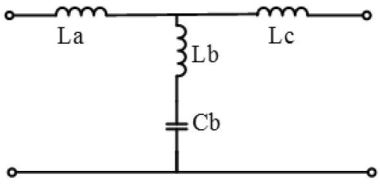

FIGURE 2 Brune section

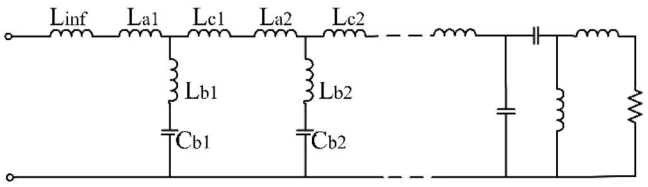

FIGURE 3 Synthesis result of the non-minimum impedance

The values of the remaining elements of the network are determined with the classical synthesis routine. Therefore, the value of $L_{\inf}$ should be set as to get positive value after summation with L_{a1}. The summation results of the remaining adjacent inductors at series arm may result with positive value. Therefore, by using trail error adjustment it is possible to eliminate all negative inductors. As our practical observations show that the Foster reactance part of back-end impedance should be bigger than the summation of negative inductors of Brune sections (i.e., $L_{\inf} > |L_{a1} + L_{a2} + \cdots|$) Therefore, the Foster part should be kept at a relatively small value, after which it should be adjusted until the elimination of each negative inductor occurs with satisfying TPG response.

4 | LOW PASS FILTER DESIGN WITH THE PROPOSED APPROACH

The outlined design procedure is easily implemented for LP filter applications. The back-end driving point impedance of an LP filter network can be determined by using the parametric design step in (1) to (10). The transmission zeros of any LP network must be placed at infinity and/or finite frequencies. Therefore, the $F(p)$ polynomial is obtained as:

$$F(p) = a_0^2 \prod_{i=1}^{n_z} \left(p^2 + w_i^2\right)^2 \tag{13}$$

After this definition, the coefficients of $c(p)$ polynomial are initiated. For transformer-free design, the a_0 parameter is set as

$$a_0 = 1/w_i^2 \tag{14}$$

Here, the Foster reactance part of the impedance is defined as a single inductor. Since the load network of filter is a unity resistor then the TPG function in (9) is modified as

$$TPG(w) = \frac{4R_G(w)}{(1 + R_G(w))^2 + (X_G(w))^2} \tag{15}$$

By using RFT optimization routine, which is summarized in Section 2, the back-end driving point impedance of a LP filter is achieved with respect to the desired TPG level.

5 | EXAMINATION OF STOP-BAND SUPPRESSION OF THE GENERATED FILTER

The introduced design approach has certain benefits in LP filter design. Starting with the degenerative driving point impedance provides a better convergence in optimization. The Foster reactance part of the driving point impedance provides superior stop band suppression in accordance with transfer function-based LP filters. The following example is given to support this claim.

In the first example, a sixth-degree driving point impedance is generated with the outlined design procedure in Sections 2–4. The performance of the filter is compared with elliptical filter. The complexity of the both filter is chosen identical. The finite transmission zeros of both filter are chosen as $w_1 = 1.0794$, $w_2 = 1.2403$, and $w_3 = 2.7163$. The elliptical filter is generated with Matlab built-in function *ellipap* [9]. The input of the *ellipap* function is $n = 6$, $Rp = 0.3$, $Rs = 30$, where n is the degree of the filter, Rp and Rs are the ripple in pass-band and stop-band. The TPG responses of the filters are given in Figure 4. The synthesis of the filter is obtained with the presented synthesis procedure and it is given in Figure 5.

As seen in Figure 4, the stop-band suppression of the proposed filter has better performance than classical elliptical filter. The filter network is also synthesized following the synthesis steps in Section 3. It can be seen that summation of values of the cascading inductors at the series arm results with all positive values.

In second example, the eighth-degree driving point impedance was generated and optimized with the proposed approach. The finite transmission zeros are placed at $w_1 = 1.0477$, $w_2 = 1.1025$, $w_3 = 1.3531$, and $w_4 = 3.2232$. The input parameters of *ellipap* filter generator function are chosen as $n = 8$, $Rp = 0.2$, $Rs = 40$. The TPG responses of the filters are given in Figure 6. The synthesis of the filter is obtained using the presented synthesis procedure and it is given in Figure 7.

Increasing the number of complexity and also changing the design parameters of the elliptical filter does not change the result. The proposed filter has a better suppression characteristic at the stop band. The synthesis result shows this filter can be realizable since cascading positive and negative inductors results in positive values.

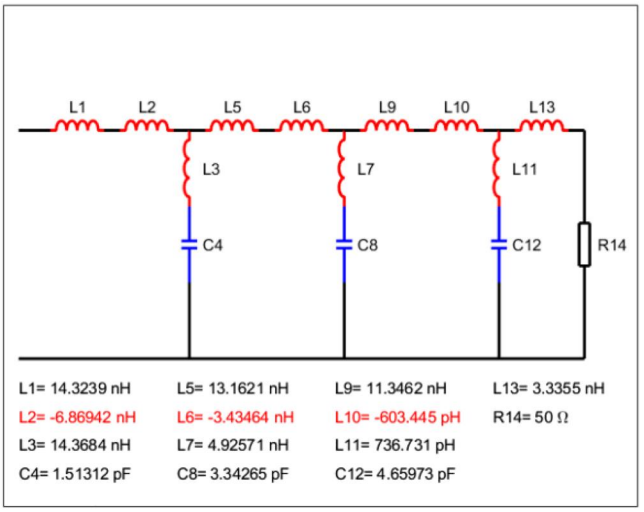

FIGURE 5 Synthesis result of the designed sixth-degree filter

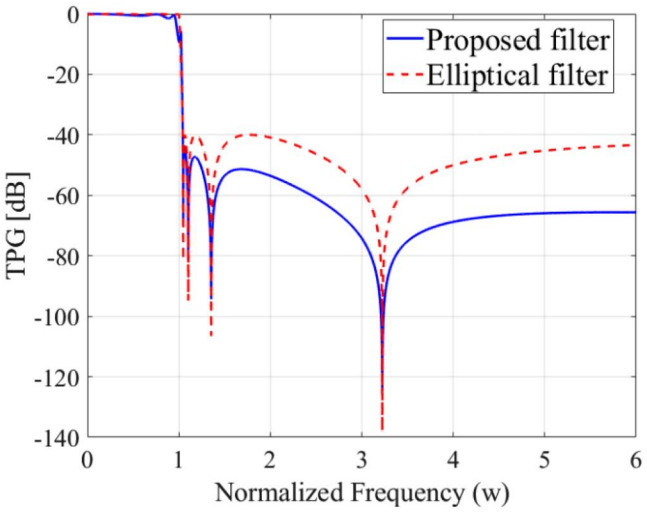

FIGURE 6 Transducer power gain of filters in eighth degree

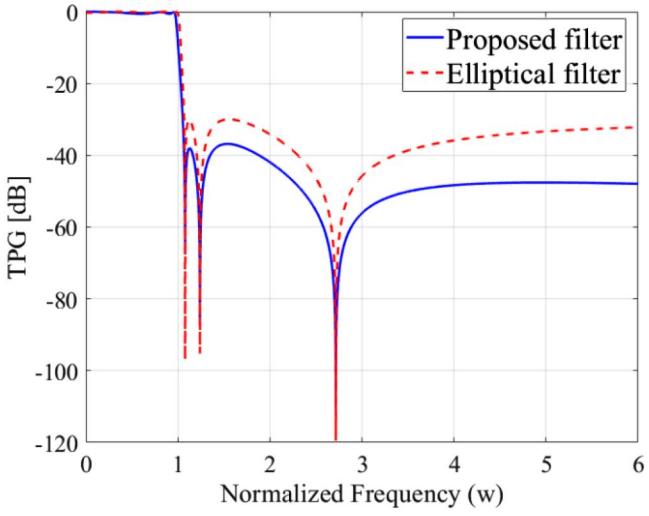

FIGURE 4 Transducer power gain of filters in sixth degree

6 | LOW PASS FILTER DESIGN AND IMPLEMENTATION

An LP filter design implementation is presented in this section. This implementation is given to validate the proposed method from practical realization aspect. For the sake of simplicity, we choose the degree of the filter as 4. The finite transmission zeros of the filter are placed at normalized frequencies

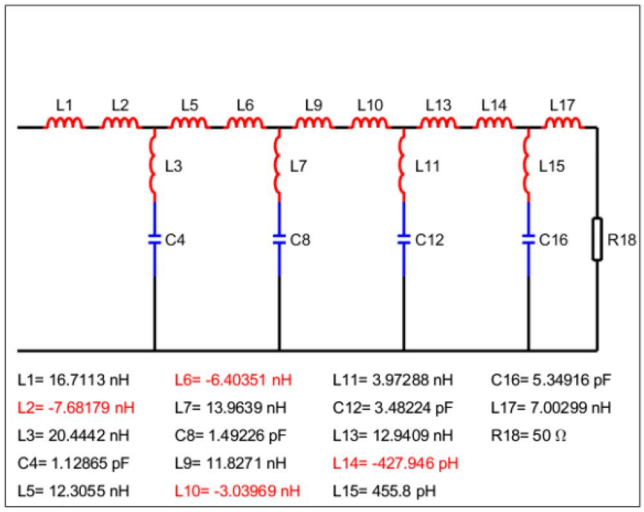

FIGURE 7 Synthesis result of the designed eighth-degree filter

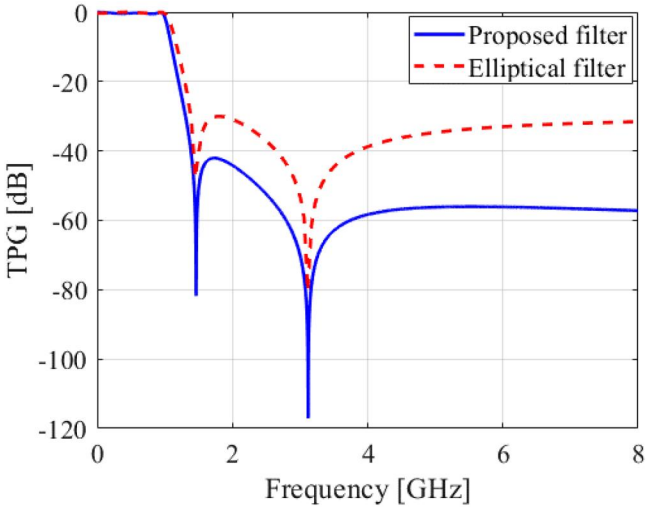

FIGURE 8 TPG performance of the designed filter and elliptical filter

TABLE 1 Component values of the prototyped filter

n(p)	d(p)
2.0000	0
1.6026	1.0000
3.4033	0.8012
1.7972	1.3180
1.3056	0.5893
0.2745	0.2745

$w_1 = 1.46$ and $w_2 = 3.1194$, which correspond to 1.46 and 3.1194 GHz, respectively. Thus the de-normalization frequency is 1 GHz. The Foster reactance part of the back-end impedance is fixed to $L_{\text{inf}} = 2$. The filter cut-off chosen as 1 GHz to prevent dielectric losses at higher frequencies.

The design steps in Section 2 are followed. The minimum part of the impedance is optimized over the normalized frequencies [0 1]in RFT routine. The coefficients of the denominator and numerator polynomials of the optimized impedance are given in Table 1.

To compare the designed filter with an elliptical filter in an identical degree, the *ellipap* function with $n = 4$, $Rp = 0.3$, $Rs = 30$ parameters is used.

The TPG performances of the designed LP filter and the elliptical filter are shown in Figure 8. As seen in the figure, the stop-band suppression performance is better than the elliptical filter correspondence. The synthesis result of the impedance function is given in Figure 9.

The cascading positive and negative valued inductors are summed up and resulted as positive valued single inductor. Thus, the synthesized filter is in realizable form.

The next step of the design involves the implementation of the designed filter. The synthesized filter is composed of lumped elements. However, lumped elements generate parasitics and losses in microwave frequencies [10]. Besides, several lumped components may not be found available vendors.

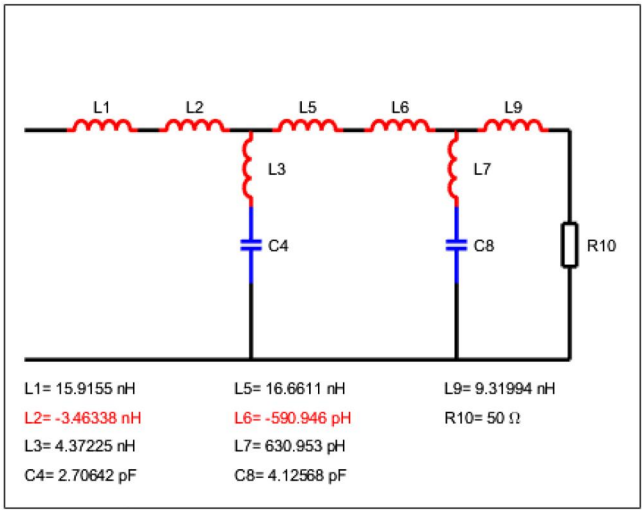

FIGURE 9 Synthesis of the designed low pass filter

Therefore, it is wise to use microstrip equivalencies of those lumped elements. However, fully microstrip topologies have their own difficulties and drawbacks [11,12]. Thus, using lumped and microstrip elements in a mixed topology have benefits of both topologies and are free of disadvantages of fully lumped or microstrip topologies [13]. For these reasons, the lumped filter in Figure 9 is converted to a mixed topology.

The final implementable filter is achieved by fine tuning of the parameters of microstrip elements and commercially available lumped components. The electromagnetic lossy model of the each component is inserted in design environment and simulations are performed. The resultant final design is printed on FR4 substrate having a relative permittivity of 4.6 and height of 1.6 mm. The layout of the final LP filter is given in Figure 10.

The component values and parameters of the microstrip elements of the layout are given on Table 2.

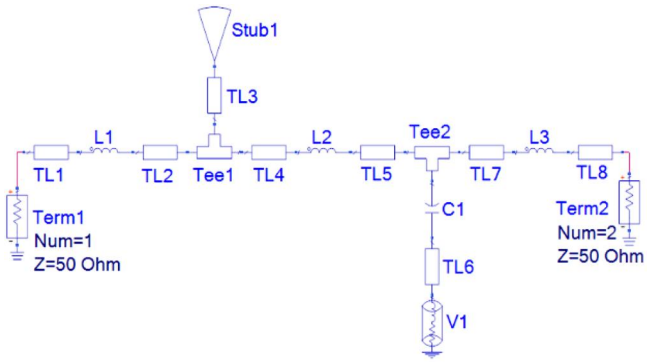

FIGURE 10 The mixed model layout of the designed low pass filter

TABLE 2 Component values of the mixed-model filter

Component names	Component specifications
L1	10 nH Murata LQW15AN10NG00
L2	16 nH Murata LQW15AN16NG00
L3	8.7 nH Murata LQW15AN8N7G00
C1	4.3 pF Murata GJM1555C1H4R3CB01
TL1,TL8	W = 3 mm, L = 15 mm
TL2, TL4, TL5, TL7	W = 0.8 mm, L = 0.5 mm
TL3	W = 0.6 mm, L = 5.52 mm
TL8	W = 0.8 mm, L = 0.5 mm
Tee1	$W1$ = 0.8 mm, $W2$ = 0.8 mm, $W3$ = 0.6 mm
Tee2	$W1$ = 0.8 mm, $W2$ = 0.8 mm, $W3$ = 0.8 mm
Stub1	L = 8 mm, Ang = 75 Deg, Wi = 0.6
V1	VIAGND D = 0.5 mm, T = 0.1 mm, W = 1 mm
PCB	FR4, h = 1.6 mm, Er = 4.6, tan ∂ = 0.02

The implemented filter is shown in Figure 11.

The insertion loss and return loss performances of the implemented filter are measured using Rohde & Schwarz ZVB14 network analyser. The measurement set-up is shown in Figure 12.

The comparison of the insertion loss and return loss performances of the implemented filter, lumped model and mixed model filters are shown in Figures 13 and 14, respectively.

The figures show that the scattering parameter performances of the lumped model, mixed model, and implemented filters are consistent with each other. The second and third pass bands in Figure 13 occur since we used chip inductors which have limited bandwidth in mixed model and implemented filters. The shift between the lumped and mixed models is due to approximations when converting the lumped elements to microstrip correspondences and using commercially available lumped elements besides theoretical values. The difference between mixed model and the implemented filter is caused by the weakness of the electromagnetic model of vendor libraries, measurement inaccuracies, dielectric losses and production tolerances.

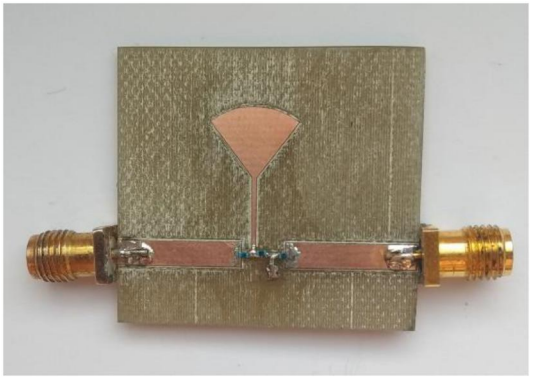

FIGURE 11 Implementation of the designed low pass filter

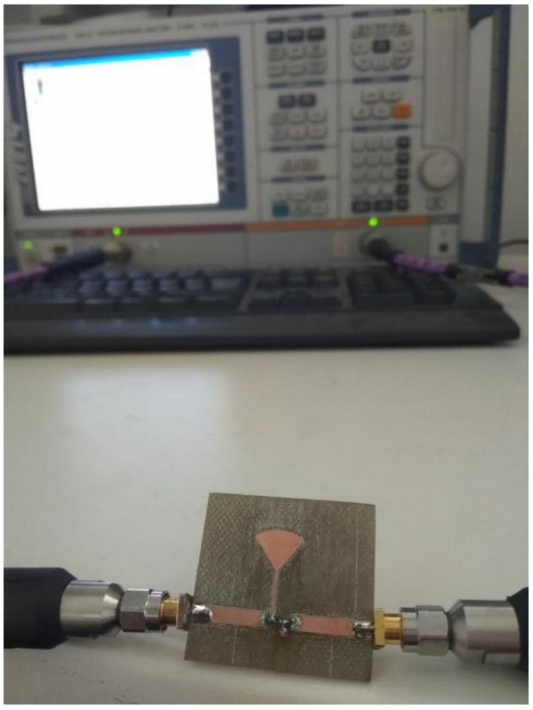

FIGURE 12 Measurement setup of the implemented low pass filter

7 | CONCLUSION

This study has investigated an LP filter design method, involving parametric representation of nonminimum back-end impedance which is composed of a minimum part and a Foster reactance part impedances. This parametric form of the impedance is used in the RFT procedure to design a realizable LP filter with assigned topology and performances characteristics. This presented design procedure is compared with the transfer function-based elliptical filters in several examples. It has been shown that the designed filters have better stop-band suppression characteristic with respect to elliptical filters in the same complexity. Moreover, the insertion loss performance at the pass band is similar. Therefore, this method enables us to design LP filters which have better stop-band suppression.

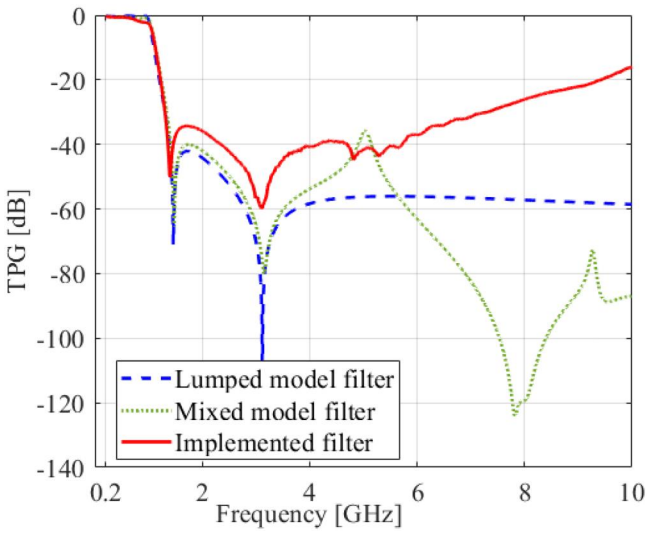

FIGURE 13 Insertion loss performance results of the lumped model, mixed model and implemented filters

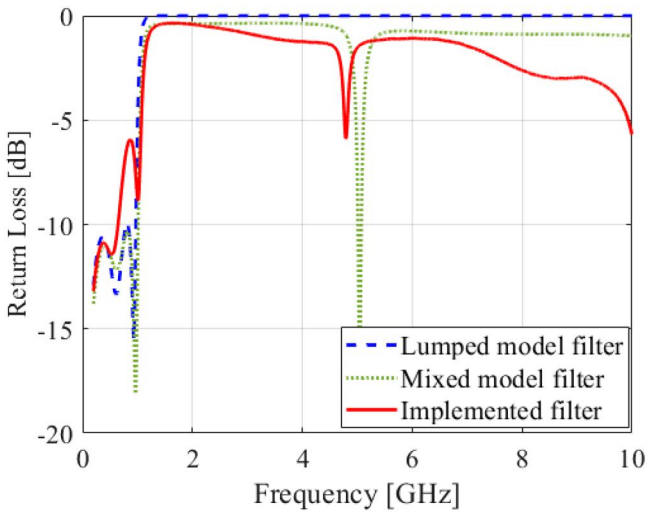

FIGURE 14 Return loss performance results of the lumped model, mixed model and implemented filters

The synthesis of the filter is performed via presented synthesis procedure. The described impedance function generally has finite transmission zeros. These are synthesized as Brune sections with negative inductors. Those negative inductors are also eliminated due to the Foster reactance section and cascading positive inductors of each Brune sections.

An LP filter design and implementation results are presented. It has been shown that the measurement results are consistent with the performance of the theoretical design. Thus the implemented filter shows that the element values of the synthesized filter are not difficult for practical realizations both in lumped and distributed domains.

ACKNOWLEDGEMENT

The authors thank Dr. Koray Gürkan and his research group in the Electronics Laboratory of Istanbul University-Cerrahpasa, for their efforts in production of the prototyped circuit.

REFERENCES

1. Pramanick, P., Bhartia, P.: Modern RF and microwave filter design. Artech House, 1, 145–201 (2016)
2. Zhu, Y.-S., Chen, W.: Low-pass impedance transformation networks. IEE Proc. Circuit. Device Syst. 144(5), 284–288 (1997)
3. Yarman, B.S.: Design of Ultra-Wideband Power Transfer Networks, 1st ed., pp. 335–389. John Wiley & Sons Ltd. UK (2010)
4. Kilinc, A., Yarman, B.S.: High precision LC ladder synthesis Part I: lowpass ladder synthesis via parametric approach. IEEE Trans Circuit. Syst. I Regular Paper. 60(8), 2074–2083 (2013)
5. Yarman, B.S., et al.: Computer aided darlington synthesis of an all purpose immittance function. IU-JEEE. 16(1), 2027–2037 (2016)
6. Fujimoto, H., Murakami, K., Kitazawa, S.: Equivalent circuits and transmission zeros of the coupled square-loop resonator. IEICE Electron. Express. 4(18), 575–581 (2007)
7. Levy, R., Whiteley, I.: Synthesis of distributed elliptic-function filters from lumped-constant prototypes. IEEE Trans. Microw. Theory Tech. 14(11), 506–517 (1966)
8. Yildiz, S., Aksen, A., Yarman, B.S.: Transformer-less ladder network design with non-minimum impedance functions. In: Conference on Electrical and Electronics Engineering, (ELECO), Bursa, Turkey, (ELECO), Bursa, Turkey, pp. 500–502 (2019)
9. MATLAB: The MathWorks, Inc. Natick, MA. (2020)
10. Almalkawi, M.J.: RF and Microwave Module Level Design and Integration: Materials, Circuits and Device. The Institution of Engineering and Technology (2019)
11. Chen, J., Xue, Q.: Compact microstrip low-pass filter with suppression of spurious response. IEE Proc Microw. Antenn. Propag. 153(5), 432–434 (2006)
12. Li, Q., Zhang, Y., Fan, Y.: Compact ultra-wide stopband low pass filter using multimode resonators. Electron. Lett. 51(14), 1084–1085 (2015)
13. Rhodes, J. D., Marston, P. C.: Cascade synthesis of transmission lines and lossless lumped networks. Electron Lett. 7(20), 621–622 (1971)

How to cite this article: Yildiz S, Aksen A, Kilinc S, Yarman SB. Low pass filter design with improved stopband suppression and synthesis with transformer-free ladders. *IET Circuits Devices Syst*. 2021;1–7. https://doi.org/10.1049/cds2.12045